Effects of out-of-band and time-varying relative spectral response on the calibration of MODIS reflective solar bands

Kevin A. Twedt,[a,*] Amit Angal,[a] Xiaoxiong Xiong,[b]
[a]Science Systems and Applications Inc., Lanham, MD 20706, USA
[b]Sciences and Exploration Directorate, NASA/GSFC, Greenbelt, MD 20771, USA

Abstract. Calibration of the on-orbit gain changes of the narrow bandwidth reflective solar bands (RSB) of Terra and Aqua MODIS is usually based on the band center wavelength. The relative spectral response (RSR) of each band is assumed to be constant on orbit and the time dependence of an overall gain factor is calculated. Any on-orbit changes to the RSR of the MODIS bands will introduce some error into the calibration and may also have an impact on the Earth scene radiance retrieval. We consider two different ways to track how the RSR of the MODIS RSB may be changing on orbit, and the effects that these changes will have on the calibration. First, we study the broadband degradation of the MODIS scan mirror and how it may be changing the effective out-of-band response of the RSB. Second, we examine in-band RSR measurements from the spectro-radiometric calibration assembly (SRCA) carried on-board both MODIS instruments. We find that RSR changes have a relatively small effect on the radiance calibrated using the on-board solar diffuser, generally less than 0.5% for all RSB at any time in the missions, though the effect may be slightly larger for some scan angles. The impact of RSR changes on the Earth scene radiance retrieval is highly dependent on the spectral properties of the scene and could be significantly larger. The bands showing the largest impacts are Terra bands 1, 4, 8, 9, 17, and 19 and Aqua bands 8 and 9.

Keywords: MODIS, reflective solar bands, spectral response

***E-mail: kevin.twedt@ssaihq.com

1 Introduction

The MODIS instruments on board the Terra and Aqua spacecraft are multi-spectral imaging radiometers that have been providing high quality Earth observations since their launches in 1999 and 2002, respectively. The sun-synchronous satellite orbits make it possible for the MODIS instruments to collect measurements of the Earth spectral radiance with full global coverage on a near-daily basis. This data record has enabled a wide array of long-term scientific and environmental data products and studies. MODIS continuously collects light in 36 spectral channels, covering both the reflected solar and thermal emissive spectral regions, using a two-sided scan mirror to image successive swaths of the Earth along the satellite track. There are several on-board calibrators (OBC) to aid in the on-orbit characterization and calibration of the

MODIS detectors, including a solar diffuser (SD) and SD stability monitor (SDSM) for calibrating the reflective solar bands (RSB), a blackbody for calibrating the thermal emissive bands, and a spectro-radiometric calibration assembly (SRCA) for monitoring spatial and spectral performance. More details of the MODIS design and operation can be found in previous publications.[1,2]

MODIS has 20 RSB with wavelengths spanning 412 nm to 2130 nm and bandwidths varying from 10 nm to 50 nm. The radiometric gains of each of the RSB were calibrated prior to launch and changes to the gains are tracked on orbit using a combination of data from the on-board SD, regular lunar observations, and pseudo-invariant desert targets.[3,4] To accurately relate the digital response of the MODIS bands to the observed Earth scene radiance and reflectance, the full spectral response of the instrument as a function of wavelength needs to be considered. The spectral response of both MODIS instruments, including both the in-band (IB) and out-of-band (OOB) components, was measured extensively prior to launch.[5] The calibration approach used by the MODIS Characterization Support Team (MCST) to generate the current NASA Collection 6 and 6.1 Level 1B (C6/6.1 L1B) products, as well as the L1B products from all previous Collections, only considers the pre-launch measured IB response and not the OOB response. The on-orbit changes in the RSB gains are calculated based on the wavelength-integrated response of each band, i.e. the relative spectral response (RSR) is assumed to be unchanged on-orbit so that the time-dependence of the spectral response of each band can be represented by a simple multiplicative factor that is independent of wavelength. These calibration assumptions have worked well due to the relatively narrow bandwidth and the relatively low OOB response of the MODIS bands.

However, the calibrated RSB gains can be impacted by the OOB RSR even if it does not change in time, due to the changing radiance of the SD as it degrades on orbit. In addition, any time-dependent on-orbit changes to the RSR of the bands will introduce some error into the calibration

and may also have an impact on the Earth scene radiance retrieval. In this paper, we present a comprehensive examination of how the in-band and out-of-band RSR, and any on-orbit changes to these quantities, impact the calibration of MODIS RSB reflectance and radiance, as well as the downstream science products. We consider two different ways to track how the RSR of the MODIS RSB may be changing on orbit, and the effect that these changes will have on the calibration. First, we consider how the broadband degradation of the MODIS scan mirror may be changing the effective OOB response of the RSB. Since launch, the gains of the RSB have experienced changes, most strongly in the blue wavelengths, primarily due to the optical degradation of the unshielded scan mirror. The wavelength and time dependent optical degradation alters the effective RSR of each of the bands. The magnitude of the effect of this modulated RSR depends on the magnitude and wavelength of the primary OOB components relative to the central band peak. This type of time-dependent modulated RSR is included in the calibration of SNPP VIIRS,[6] a follow-on instrument to MODIS that has a very similar design, and has also recently been included in the calibration of Aqua MODIS band 8 in the NASA ocean color products.[7,8]

Second, we examine measurements from the SRCA carried on-board both MODIS instruments. The SRCA is a unique calibrator that was designed to track the radiometric and spectral performance of the MODIS RSB on orbit, as well as the spatial performance of all MODIS bands (RSB and thermal emissive bands). The SRCA has provided direct measurements of the IB RSR of most RSB multiple times per year since launch.[9–13]

In Section 2, we review the pre-launch measured IB and OOB RSR for the MODIS RSB and consider how the pre-launch OOB RSR affects the on-orbit calibration. In Section 3, we present the methodology for calculating the impact of a time-dependent RSR on the calibration of the reflectance and radiance. In Section 4, we review the degradation of the RSB determined using

our current calibration methodology and attempt to separate the optical degradation of the scan mirror from other instrument effects. We then calculate the modulated RSR and the impact on the calibrated radiance. We focus initially on the impact of time-dependent RSR on the SD-based calibration. Then in Section 5, we look at the differences in the results at different scan angles and when using lunar and desert calibration sites, which are needed for characterization of the on-orbit response versus scan angle (RVS) function. Section 6 provides a discussion on the implications for Earth scene radiance retrieval as well as a methodology for including a time-dependent RSR in the L1B product, which can be considered for inclusion in future MODIS Collections. In Section 7, we present IB RSR measurements from the SRCA spectral calibrations and estimate the impact that these changes may have on both the calibration and the Earth scene products. Since the SRCA only measures the IB portion of the RSR and we have no way to merge this with the OOB RSR, it would be difficult to use the SRCA measurements to adjust the L1B calibration in a rigorous quantitative way, but they still provide important insight on the impact of on-orbit RSR changes, especially for Terra MODIS. Section 8 gives a brief summary.

In general, we find that including the OOB and time-dependent RSR alters the long-term trends of the SD-based calibrated radiance by up to 0.5% in the worst cases and much less for most RSB, though the impact may be slightly larger at other scan angles. The largest RSR impacts are seen for Terra MODIS bands 1, 4, 8, 9, 17, and 19 and Aqua MODIS bands 8 and 9. The impact on the retrieved Earth scene radiance is highly dependent on the spectral properties of the scene and could be up to a few percent for example in the water absorption band 19 of Terra MODIS when viewing a typical cloud spectral profile. There is considerable uncertainty in these results due both to the uncertainty in the normalization of the pre-launch OOB RSR measurements (see Section 2) and to the assumptions that need to be made to perform the on-orbit analyses. Since there is no way to

directly measure OOB RSR changes on-orbit, our results should be viewed only as an estimate of the RSR's potential impact. Nevertheless, the data indicate that the L1B product quality for both MODIS instruments is not significantly affected by on-orbit RSR changes.

The results in this paper focus mainly on the VIS/NIR bands and not the SWIR bands. The OOB RSR for the SWIR bands (HgCdTe detectors) and the VIS/NIR bands (Si detectors) generally do not overlap, so on-orbit changes in the VIS/NIR wavelength range will not impact the SWIR bands, and vice versa. Also, the SWIR bands have had known issues since launch with large OOB response in the mid-wave IR wavelength range as well as electronic crosstalk effects[14,15] which complicate any on-orbit RSR analysis.

2 Pre-launch RSR

2.1 Pre-launch RSR measurements

Both the in-band and out-of-band spectral responses of all MODIS detectors were measured during pre-launch testing.[5] The IB spectral responses were measured during the thermal vacuum testing phase using a spectral measurement assembly (SpMA), which consisted of broadband filters and a double grating monochromater to scan the spectral response of each detector. Table 1 lists the measured center wavelength and bandwidth of the center detector of each MODIS RSB. The bandwidth is the full width half maximum of the in-band RSR and the center wavelength is the mid-point between the half maximum points. The MODIS OOB responses were also characterized using the SpMA, but with a larger exit slit in order to increase the amount of light reaching the detectors. As a result, the OOB response curves need to be separately normalized before combining with the IB response curves. The OOB and IB RSR measurements were combined together and a final merged IB/OOB pre-launch RSR was provided for all RSB by the MODIS instrument vendor,

Santa Barbara Remote Sensing. For Aqua MODIS, however, two preliminary versions of the merged RSR were provided, which we refer to as method 1 and method 2, the difference coming from the method of normalization of the OOB response curves. Rather than re-analyze the pre-launch data to determine which of the two methods is preferable, we present results from both methods in this paper. The difference between the two gives an indication of the amount of uncertainty in the pre-launch RSR and how it might impact the MODIS calibration.

Table 1. Center wavelengths and bandwidths of the MODIS RSB from pre-launch measurements.

Band	Center Wavelength (nm)		Bandwidth (nm)		Band	Center Wavelength (nm)		Bandwidth (nm)	
	Terra	Aqua	Terra	Aqua		Terra	Aqua	Terra	Aqua
1	645.2	644.9	48.0	47.6	11	529.8	530.2	12.0	12.0
2	856.9	857.3	38.4	38.1	12	547.0	547.4	10.3	10.4
3	465.8	466.1	18.8	18.9	13	665.7	666.0	10.1	10.1
4	553.8	554.0	19.8	19.8	14	677.1	677.7	11.3	11.4
5	1242.1	1241.6	24.0	23.0	15	746.7	746.9	9.9	9.8
6	1629.5	1628.1	28.5	27.7	16	866.5	867.0	15.5	15.5
7	2113.7	2113.4	53.1	53.1	17	904.3	904.5	35.0	35.0
8	411.5	412.2	14.8	14.4	18	935.7	936.4	13.6	13.6
9	442.1	442.3	9.7	9.7	19	935.6	935.7	46.1	46.7
10	487.1	487.5	10.6	10.7	26	1383.6	1383.7	35.0	36.7

Figure 1 shows the combined IB and OOB pre-launch RSR for all RSB for Terra MODIS and Aqua MODIS method 1. The data in Table 1 and Figure 1 show that Terra and Aqua MODIS in general have very similar spectral responses. The magnitude of the OOB RSR at wavelengths away from the band central wavelength is largest for Aqua MODIS band 8 (412 nm), where it exceeds 1% around 510 nm. For the SWIR bands of both instruments, pre-launch measurements also showed large OOB optical leaks in the mid-wave IR, centered around 5300 nm, that are not shown in Figure 1. Figure 2 shows a comparison of the two different RSR methods for Aqua bands 8 and 9. We focus on bands 8 and 9 since they have some of the largest differences in OOB RSR between the two methods and also show the greatest impact to the on-orbit calibration, as we show in the following Sections. Note that the large OOB peak around 510 nm for band 8 is nearly an order of magnitude smaller for method 2 compared to method 1.

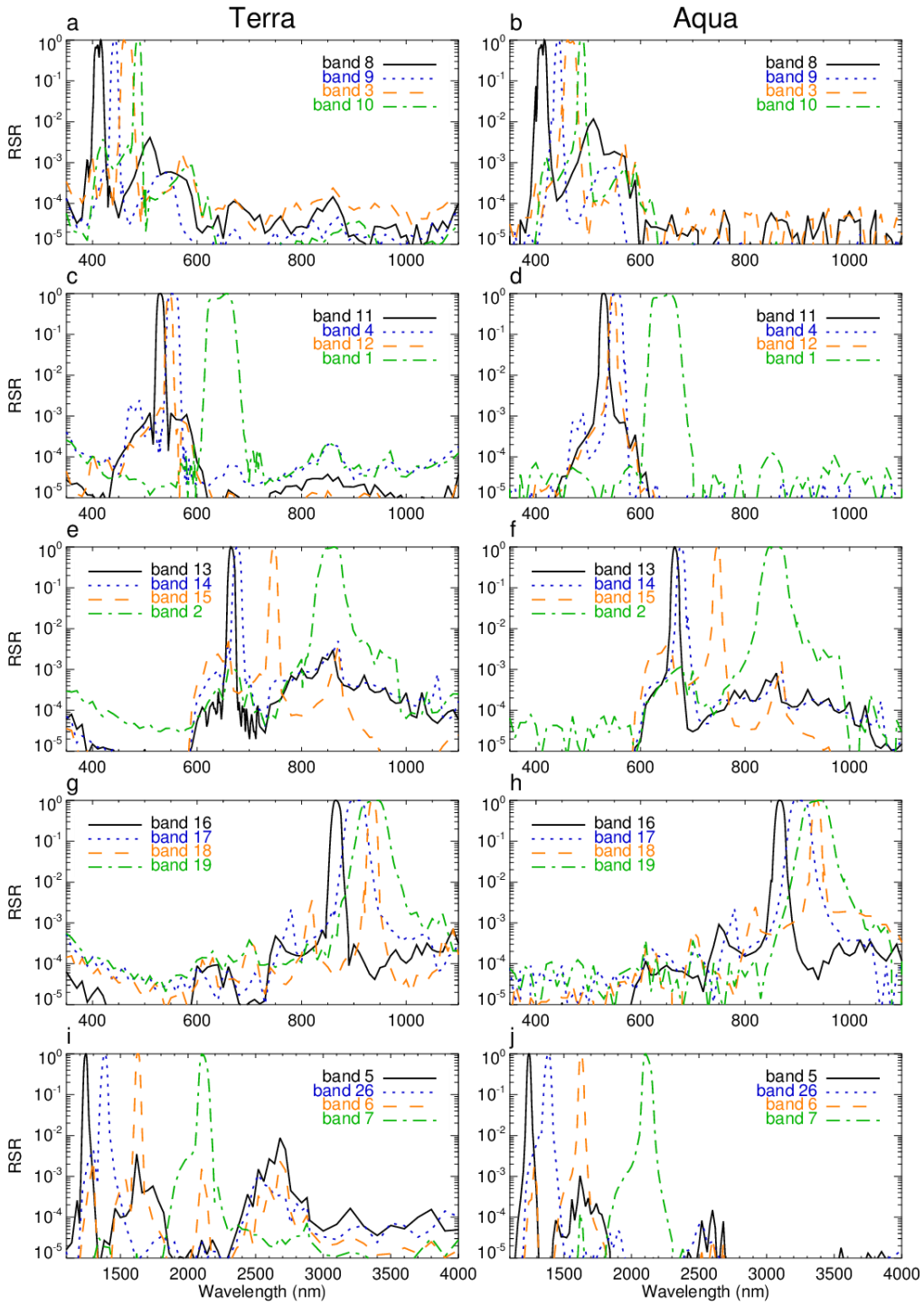

Fig. 1. Merged pre-launch IB and OOB RSR measurements for Terra (a,c,e,g,i) and Aqua (b,d,f,h,j) MODIS RSB.

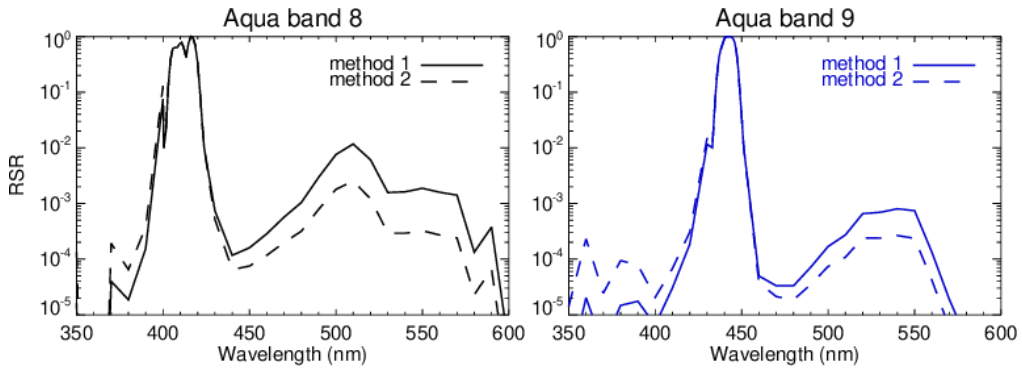

Fig. 2. Comparison of merged pre-launch IB and OOB RSR measurements for the two different merging methods for Aqua MODIS bands 8 (left) and 9 (right) over the visible spectral range.

The calibrated MODIS L1B products have used the pre-launch measured IB RSR since the beginning of the MODIS missions, where the in-band response is defined as the response around the band center wavelength above 1% of the peak response. However, the pre-launch OOB RSR measurements have not been used in the L1B products or any of the calibration algorithms used to date by the MCST. Here, we review the basic SD-based calibration methodology of the MODIS RSB and we consider how the calibrated results are changed if the merged pre-launch IB/OOB RSR measurements are used in the calculations.

The primary products of the MODIS RSB are the top-of-atmosphere (TOA) reflectance factor, defined as

$$\rho_{EV}\cos(\theta_{EV}) = m_1 dn^*_{EV} d^2_{ES}/RVS_{EV}, \quad (1)$$

and the radiance, defined as

$$\overline{L_{EV}} = \frac{\rho_{EV}\cos(\theta_{EV})\overline{E_{sun}}}{\pi d^2_{ES}} = \frac{m_1 dn^*_{EV}\overline{E_{sun}}}{\pi RVS_{EV}}, \quad (2)$$

where dn^*_{EV} is the digital response of each Earth view (EV) pixel corrected for background and instrument temperature variations, d_{ES} is the Earth-Sun distance in astronomical units (AU), m_1 is a calibration coefficient, and RVS_{EV} is the response versus scan angle of the instrument at the angle of the EV pixel. The $\overline{E_{sun}}$ term is the solar spectral power per steradian at 1 AU integrated

over the RSR of each MODIS detector. MODIS uses a fixed solar spectral profile that is the combination of three sets of historical measurements to cover the entire reflected solar portion of the spectrum. Terra and Aqua have both been in orbit long enough to observe nearly two full solar cycles, but the short-term and long-term variations of the absolute solar spectral power over this time are relatively small and are not considered here. The bar notation on $\overline{E_{sun}}$ and $\overline{L_{EV}}$ is used throughout to indicate that the radiance measured by a MODIS band is always the spectral radiance at the MODIS entrance aperture integrated over the relative response of the band, defined as

$$\overline{L_{scene}}(B) = \frac{\int RSR(\lambda,B) L_{scene}(\lambda) d\lambda}{\int RSR(\lambda,B) d\lambda}, \tag{3}$$

and

$$\overline{E_{sun}}(B) = \frac{\int RSR(\lambda,B) E_{sun}(\lambda) d\lambda}{\int RSR(\lambda,B) d\lambda}, \tag{4}$$

where B and λ are used to distinguish between band and wavelength dependence.

In the L1B products, only the in-band RSR is used in calculating $\overline{E_{sun}}$ for the L1B radiance. The RSR (and $\overline{E_{sun}}$) is considered to be constant in time and has not been updated on orbit. Throughout the rest of this paper, we use the full pre-launch IB/OOB RSR in all calculations, and in Sections 3-7 we allow the RSR and thus the $\overline{E_{sun}}$ term to vary in time. As a result, the value of $\overline{E_{sun}}$ and thus the absolute radiance values calculated will be slightly offset from the current C6/C6.1 L1B values even at the beginning of the missions. The relative difference between $\overline{E_{sun}}$ calculated with the merged IB/OOB RSR compared to the $\overline{E_{sun}}$ values in the C6/6.1 L1B is shown in Fig. 3 for all VIS/NIR detectors of Terra and Aqua MODIS. The differences are less than 0.5% for all RSB with the exceptions of Terra band 13 (0.6%), Terra band 14 (0.7%), and Aqua band 8 (0.7% or 1.5%). The differences between detectors within a band are in general negligible. While there are separate IB RSR measurements for each detector within a band, only one band-averaged

OOB RSR was provided for each band, though in reality there may be differences between detectors that are not captured here.

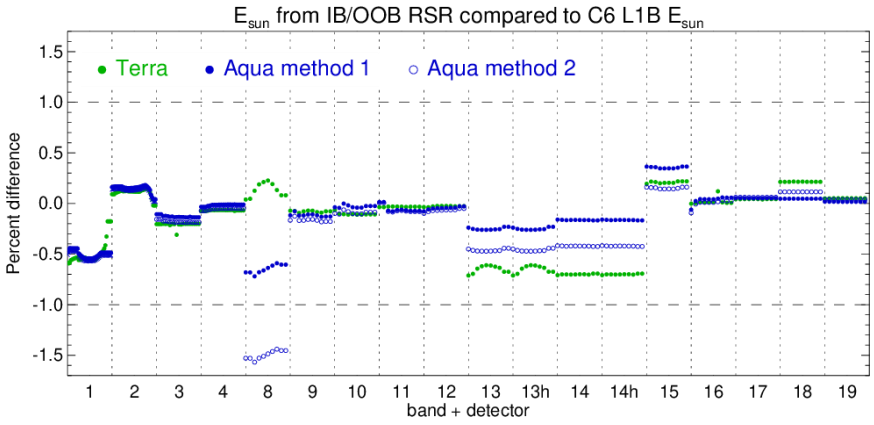

Fig. 3. Differences in percent between $\overline{E_{sun}}$ calculated with the merged IB/OOB RSR compared to the $\overline{E_{sun}}$ values in the current C6/6.1 L1B, calculated as $\overline{E_{sun}}(IB/OOB)/\overline{E_{sun}}(C6) - 1$.

2.2 Effect of pre-launch OOB RSR on SD calibration

We consider the effect of including the full pre-launch RSR in the calculation of the SD calibration. The pre-launch IB RSR was used in calculating the pre-launch band-averaged values of the SD bi-directional reflectance distribution function (BRDF) for each band, but the RSR (pre-launch or on-orbit change) is not currently used in the MCST algorithm for calculating on-orbit changes to the reflectance calibration coefficient m_1. Even though in this Section we consider the RSR to be constant in time, there will still be a time-dependent effect on the SD calibration, due to the changing radiance (i.e. degradation) of the SD on orbit.

The reflectance calibration coefficient is typically defined from the solar diffuser calibration as

$$m_1(B) = \frac{\rho_{SD}(B)\cos(\theta_{SD})}{dn^*_{SD}(B)d^2_{ES}}\Gamma_{\mathrm{SD}}\Delta_{\mathrm{SD}}(B), \quad (5)$$

where ρ_{SD} is the BRDF of the solar diffuser measured pre-launch, Γ_{SD} is the vignetting function of the solar diffuser screen, Δ_{SD} is the on-orbit degradation of the SD reflectance, dn^*_{SD} is the

background and temperature corrected digital response of the SD sector, and θ_{SD} is the angle between the solar vector and the normal of the SD surface. Using Eqs. 2-3, we can re-define the calibration coefficient for SD calibration including the RSR by considering the scene radiance to be the radiance of the SD, giving

$$m_1(B) = \frac{\cos(\theta_{SD})\Gamma_{SD}\rho_{SD}(B)\int RSR(\lambda,B)\Delta_{SD}(\lambda)E_{sun}(\lambda)d\lambda}{dn^*_{SD}(B)d^2_{ES}\int RSR(\lambda,B)E_{sun}(\lambda)d\lambda}. \quad (6)$$

In Eqs. 5-6, we use B to denote the terms that are band-dependent. Of course, several of the terms also depend on detector, sub-frame, and scan mirror side, and ρ_{SD} and Γ_{SD} depend on the incoming solar vector direction. We exclude these details from the equations for clarity. The wavelength dependence of ρ_{SD} is very small, so for simplicity we have taken this term outside the integral and use the band-average $\rho_{SD}(B)$.

In the case where there is no wavelength-dependent degradation of the SD reflectance (i.e. Δ_{SD} does not depend on λ), then Eq. 6 reduces to the usual Eq. 5. However, the SD reflectance degradation does depend on wavelength, and this causes the calibrated gain calculated with Eq. 6 to diverge from the usual calibrated gain calculated with Eq. 5. We calculate these two quantities over the course of the mission for both Terra and Aqua. The ratio of the results is presented in Fig. 4. The SD degradation that we use is determined from a time-series fitting of the results from SDSM measurements, which have been extensively described in previous work.[16]

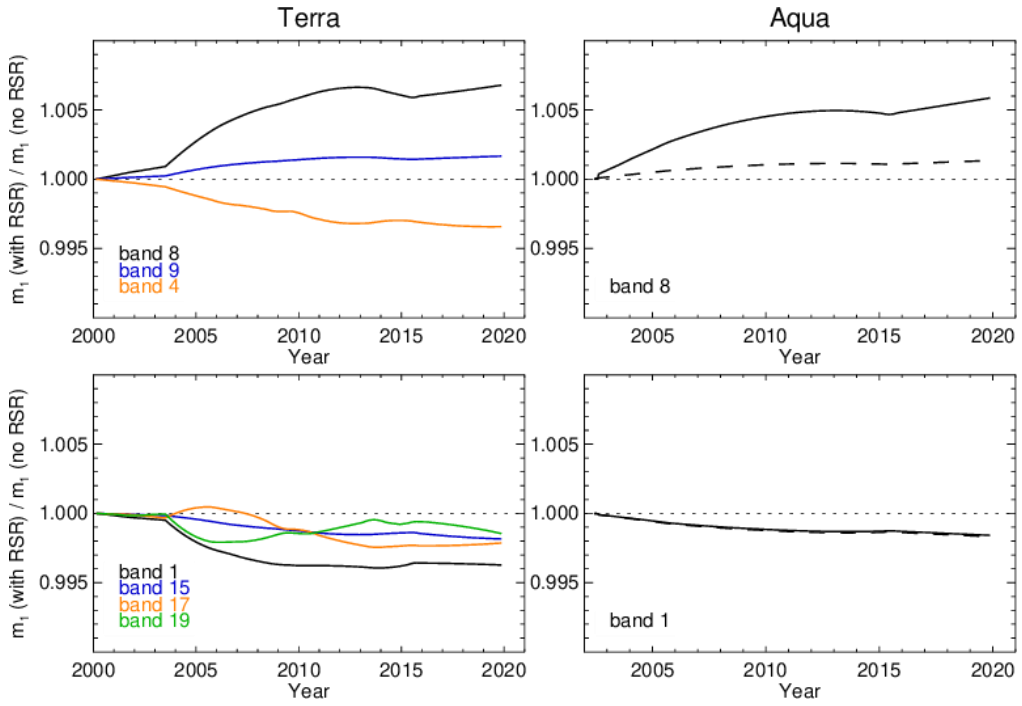

Fig. 4. Relative impact of the pre-launch OOB RSR on m_1 over the missions for (left) Terra and (right) Aqua MODIS RSB. Only bands that show changes greater than 0.15% are shown. For Aqua, the solid lines and dashed lines correspond to method 1 and method 2, respectively.

For Aqua MODIS, band 8 shows the largest difference of up to 0.6% for method 1 and 0.15% for method 2, whereas all other bands are about 0.15% or less. It is not surprising that the impact is largest for band 8 (412 nm) as the SD degradation is greatest at the lower wavelengths and band 8 has a relatively large OOB RSR. For Terra MODIS, band 8 also sees the largest on-orbit effect of up to 0.6%, and the rest of the VIS/NIR bands in general show a larger effect of the RSR compared to Aqua MODIS. Terra MODIS is more significantly affected mostly because the on-orbit degradation of the SD has been more significant.[16] These results show the changes that would result from including the pre-launch IB/OOB RSR with no on-orbit updates in the calculation of the calibrated reflectance from the SD calibration.

The time-dependence shown in Fig. 4 results from the fact that the radiance of the calibration scene (the SD) is changing in time. There is no analogous effect for calibration done with the Moon

or pseudo-invariant desert targets. In the C6/6.1 L1B products for Terra bands 1-4, 8-10 and Aqua bands 1-4, 8-9, the long-term on-orbit gain changes are calculated using the Moon and desert targets, rather than the SD, though the SD is still used as the at-launch reference and for tracking short-term and detector dependent gain changes. Considering this, the largest effect of excluding RSR in the current m_1 calibration will be for the Terra NIR bands, which see up to 0.3% effect. In total, including the time-independent IB/OOB RSR in the calibration of the MODIS RSB would result in on-orbit reflectance and radiance drifts of up to 0.3% and absolute radiance offsets of up to 0.7% (1.5% for Aqua method 2 band 8) compared to the current C6/C6.1 L1B products.

3 Time-dependent RSR methodology

We next consider how time-dependent changes in the RSR that happen on-orbit can influence the calibration of the reflectance and radiance. We briefly set up a general methodology and then use this in the following sections to evaluate the impact of the changing broadband and in-band RSR. The baseline for the time-dependent RSR is the assumption that the at-launch RSR is equivalent to the merged IB/OOB RSR from the pre-launch measurements.

If the RSR is changing on-orbit, the calibrated radiance product and solar spectral power terms as defined in Eqs. 1-4 will also have a corresponding time dependence. We redefine $\overline{L_{scene}}$ as

$$\overline{L_{scene}}(B,t,\theta_{scan}) = \frac{\int RSR(\lambda,B,t,\theta_{scan}) L_{scene}(\lambda,t,\theta_{scan}) d\lambda}{\int RSR(\lambda,B,t,\theta_{scan}) d\lambda}, \quad (7)$$

where θ_{scan} is the viewing angle of the EV pixel within the MODIS scan. There are large variations in on-orbit RSB gains as a function of the angle of incidence (AOI) of light off the primary scan mirror, which will be an important consideration when examining the impact of the broadband RSR on the RVS calibration, discussed in Section 5. Because of this, the RSR is allowed to have a view angle dependence in addition to the time-dependence. A similar equation can be written for

$\overline{E_{sun}}$. Since the on-orbit changes to the RSR will only have a small impact on the overall calibration, we focus on calculating the relative change in the calibrated radiance calculated when using the time-dependent RSR compared to the at-launch RSR. This can be expressed as the ratio of Eq. 7 to Eq. 2:

$$R_{rad,scene}(B,t,\theta_{scan}) = \frac{\int RSR(\lambda,B,t,\theta_{scan})L_{scene}(\lambda,t,\theta_{scan})d\lambda \,/\, \int RSR(\lambda,B,t,\theta_{scan})d\lambda}{\int RSR_{pl}(\lambda,B)L_{scene}(\lambda,t,\theta_{scan})d\lambda \,/\, \int RSR_{pl}(\lambda,B)d\lambda}, \quad (8)$$

where RSR_{pl} is the merged IB/OOB pre-launch RSR. This represents the impact that the time-dependence of the RSR has on the radiance, or equivalently the error that exists in the calibration if the time-dependence of the RSR is not included. In a similar way, the ratio of the calibrated reflectance with time-dependent RSR compared to pre-launch RSR is calculated as

$$R_{refl,scene}(B,t,\theta_{scan}) = \frac{\int RSR(\lambda,B,t,\theta_{scan})L_{scene}(\lambda,t,\theta_{scan})d\lambda \,/\, \int RSR(\lambda,B,t,\theta_{scan})E_{sun}(\lambda)d\lambda}{\int RSR_{pl}(\lambda,B)L_{scene}(\lambda,t,\theta_{scan})d\lambda \,/\, \int RSR_{pl}(\lambda,B)E_{sun}(\lambda)d\lambda}. \quad (9)$$

Since R_{rad} typically has a larger deviation from unity than R_{refl}, we focus on the radiance calculations in the following analyses, but both the radiance and reflectance are impacted by the time-dependent RSR and the magnitude of the impact is heavily dependent on the spectral properties of the scene being observed.

The on-orbit calibration procedure using the SD can be evaluated in the same way as in Section 2. The impact of the time-dependent RSR on the SD radiance is

$$R_{rad,SD}(B,t) = \frac{\int RSR(\lambda,B,t)\Delta_{SD}(\lambda,t)E_{sun}(\lambda)d\lambda \,/\, \int RSR(\lambda,B,t)d\lambda}{\int RSR_{pl}(\lambda,B)\Delta_{SD}(\lambda,t)E_{sun}(\lambda)d\lambda \,/\, \int RSR_{pl}(\lambda,B)d\lambda}, \quad (10)$$

which is equivalent to the ratio of $m_1\overline{E_{sun}}$ with time-dependent RSR compared to pre-launch RSR. We have dropped the θ_{scan} dependence since the SD calibration is always performed at a single fixed scan angle. These equations will be used to evaluate the impact of the measured on-orbit changes in the RSR.

4 On-orbit Changes to Broadband RSR

4.1 On-orbit total gain changes

We now examine the effect of changes in the broadband optical throughput of the MODIS instruments on the RSR of each band, and the impact on the calibration. First, consider how the calibrated gain of the instrument has changed on-orbit. The total on-orbit gain change at the AOI of the SD, $G_{total} = m_1(t_0)/m_1(t)$, as a function of band center wavelength for Terra and Aqua MODIS at select times in the mission is shown in Fig. 5 (top row). The m_1 values in Fig. 5 are from a reprocessed calculation that uses the same algorithm as the C6.1 L1B product for most bands, with a few algorithm improvements included for Terra MODIS.[17,18] Clearly, both instruments have experienced significantly more degradation in the visible wavelength range compared to the NIR.

The MODIS scan mirror is the primary unshielded optic for MODIS and it is assumed that the majority of the instrument degradation is due to degradation of the scan mirror. This is further evidenced by a clear gain dependence on the AOI of the light on the scan mirror (the RVS). Under the assumption that the gain changes are dominated by changes to the scan mirror (and other optical elements that are in the portion of the optical path shared by all bands), then all bands will experience a broadband optical degradation. This broadband degradation can be multiplied by the pre-launch measured OOB RSR of each detector in order to provide an on-orbit update to the OOB RSR.

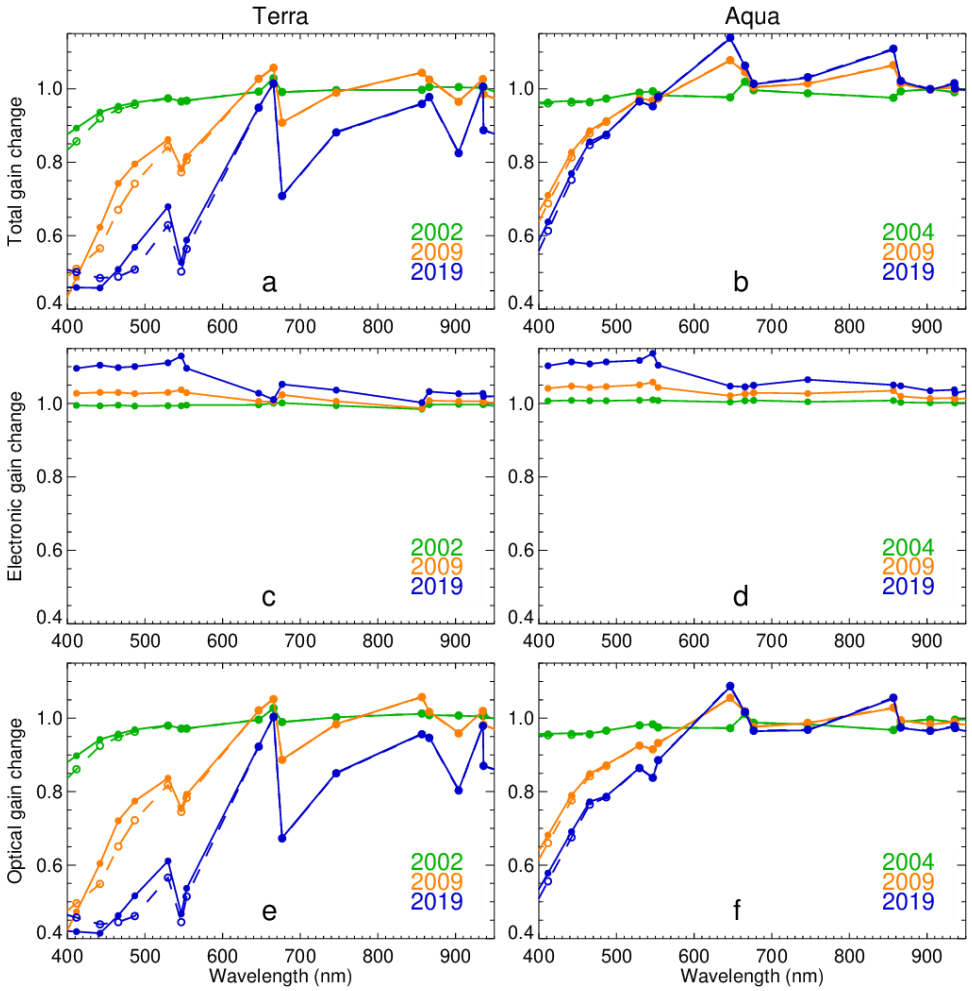

Fig. 5. On-orbit total gain (top row), electronic gain from E-cal measurements (middle row) and optical gain (bottom row) for Terra (left) and Aqua (right) MODIS VIS/NIR bands at select years during the mission. For the total and optical gain changes, both mirror side 1 (solid line and filled symbols) and mirror side 2 (dashed line and open symbols) results are shown.

4.2 Isolating the scan mirror degradation

For this approach to work, we must first isolate the degradation of the scan mirror from that of other optical and electronic components that may experience on-orbit changes and contribute to the gain degradation seen in Fig. 5a and 5b. We can consider the total gain change to be composed of changes in electronic gain, G_{elec}, detector gain, G_{det}, reflectance of the scan mirror and primary

optics, $\rho_{primary}$, reflectance of dichroic elements and focusing optics specific to each focal plane assembly (FPA), ρ_{fpa}, and the transmittance of the narrow band filters, T_{filter}, giving

$$G_{total}(B,D,S,M) \propto G_{elec}(B,D,S) \int G_{det}(\lambda,B,D,S)\, \rho_{primary}(\lambda,M)\rho_{fpa}(\lambda,FPA)T_{filter}(\lambda,B,D)d\lambda, \quad (11)$$

where we have specified the dependence of each term on the band (B), detector (D), sub-frame (S), and mirror side (M), and it is assumed that all quantities can change with time.

Fortunately, the MODIS instruments are equipped with the capability to monitor the changes in G_{elec} through on-orbit electronic calibrations (E-cals) that have been performed on a regular basis for both instruments since launch. During an E-cal, the MODIS detectors are detached and replaced by a voltage ramp that is applied during the time of space view sector data collection. The change in measured dn in response to the voltage ramp is used to calculate the electronic gain, and monitor changes in this gain on orbit. More details on the MODIS E-cals can be found in previous publications.[19]

Figure 6 shows the G_{elec} for an example band over the course of the Terra and Aqua missions. For all Aqua and Terra MODIS bands, the G_{elec} is found to increase gradually over the mission. For each band, we fit the on-orbit electronic gain change (averaged over all detectors within a band) to a polynomial function of time to derive smooth trends. Figures 5c and 5d show the electronic gain change as a function of band wavelength at select times in the missions. All of the VIS bands (wavelength less than 600 nm) have very similar changes in electronic gain, which may be related to the fact that these bands all share the same analog-to-digital converter (ADC). The NIR bands also show consistent trends and generally have less change on orbit than the VIS bands. The NIR bands are split between three ADCs, one for band 1 (645 nm), one for band 2 (858 nm) and one for the rest of the NIR bands.

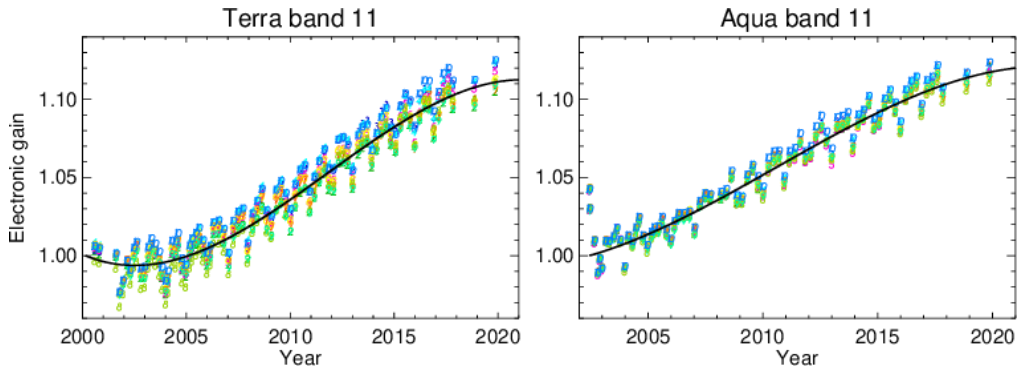

Fig. 6. On-orbit electronic gain change of Terra (left) and Aqua (right) MODIS band 11. For each calibration time, different colored/numbered symbols indicate the results of different detectors, showing the spread in the results over all detectors in the band. The black line is a polynomial fit to the results averaged over all detectors.

Considering only the average values over all detectors and sub-frames within a band, we can use the E-cal data to remove the electronic component of the on-orbit gain change and write the optical gain of the instrument as

$$G_{optical}(B,M,t) = \frac{G_{total}(B,M,t)}{G_{elec}(B,t)}. \quad (12)$$

Figures 5e and 5f show the calculated values of $G_{optical}$ as a function of wavelength. If this optical gain change were entirely due to degradation of the scan mirror, our expectation is that this would be a smooth function of wavelength, without any sharp features in the spectrum. This is mostly true for Aqua MODIS in Fig. 5f, but notably bands 1 (645 nm) and 2 (858 nm) have considerably higher gain and still see an increase in $G_{optical}$ on orbit. As it is quite unlikely that the optical throughput of the instrument has increased at any wavelength on orbit, the on-orbit trends in the gains of bands 1 and 2 likely come from a systematic effect not yet identified.

Clearly, the optical degradation of the Terra MODIS instrument as a function of wavelength in Fig. 5e carries significantly more features than Aqua MODIS. It is still likely that the degradation of the scan mirror is the primary cause of the drop in gain for Terra RSB on-orbit. But there are several features in Fig. 5e that must have a different explanation, for example the large

difference in gain between bands that have a similar wavelength, such as bands 11 (531 nm) and 12 (551 nm), or bands 13 (667 nm) and 14 (678 nm).

The $G_{optical}$ in Figs. 5e and 5f still includes the integrated effects of the detector gain and filter transmittance, in addition to the reflectivity of the optics (see Eq. 11). Any on-orbit changes in G_{det}, T_{filter}, or ρ_{FPA}, none of which we can independently measure, could influence the shape of the calculated $G_{optical}$ curves in unknown ways. All of the VIS/NIR bands use Si detectors that likely degrade in a similar way. It is known that these detectors experience gain degradation under radiation exposure initially in the NIR wavelengths. The relatively stable on-orbit performance of the NIR bands (e.g. 17-19, especially for Aqua MODIS) indicates that the Si detectors have not experienced any major radiation damage on orbit, thus it is likely that G_{det} is fairly stable on orbit for all VIS/NIR bands. The SRCA spectral results (see Sec. 7) provide some indication of the performance of the filter transmittance T_{filter} though the SRCA only measures changes in the relative and not absolute transmittance. For Aqua MODIS, which shows no significant change in the in-band RSR on orbit, it seems reasonable to assume that the band filters have not experienced significant degradation. For Terra MODIS, which does show significant change in the in-band RSR for e.g. bands 1, 4, 17, and 19, the absolute filter transmittance may very possibly also be decreasing in these bands, which may explain some of the sharp differences in on-orbit gain seen in Fig. 5e.

4.3 Impact on calibrated radiance

With the considerations discussed above, we can reasonably assume that the optical degradation for Aqua MODIS shown in Fig. 5f is dominated by the degradation of the primary scan mirror, with the exception of bands 1 and 2. The wavelength-dependent degradation can be applied to the pre-launch relative spectral response of all bands equally in order to derive a broadband time-

dependent RSR for each RSB. For Terra MODIS, this assumption is clearly less reliable, but we present an analysis for both instruments for completeness.

We define the on-orbit modulated RSR to be

$$RSR_{broadband}(\lambda, B, t) = \frac{RSR_{pl}(\lambda,B)G_{optical}(\lambda,t)}{\max_{\lambda}[RSR_{pl}(\lambda,B)G_{optical}(\lambda,t)]}, \quad (13)$$

where $G_{optical}$ is interpolated between bands to get a continuous function of wavelength. We determine the effect of the changing on-orbit RSR on the calibrated radiance of the SD calibration, $R_{rad,SD}(B,t)$, using the RSR from Eq. 13 and plot the results in Fig. 7. For both instruments, the on-orbit impact is up to 0.5% for band 8, up to 0.1% for band 9, and negligible for all other bands. For Terra MODIS, the irregularities in Fig. 5e place a great deal of uncertainty on these results, and a better understanding of the source of these gain changes is needed to provide a confident analysis. For Aqua band 8, the impact using the method 2 RSR is up to 0.3%, slightly lower than for the method 1 RSR. A similar analysis on the calibration impact of broadband RSR changes was recently published for the Aqua MODIS ocean color bands using the method 1 RSR,[7] and we find good agreement with those results.

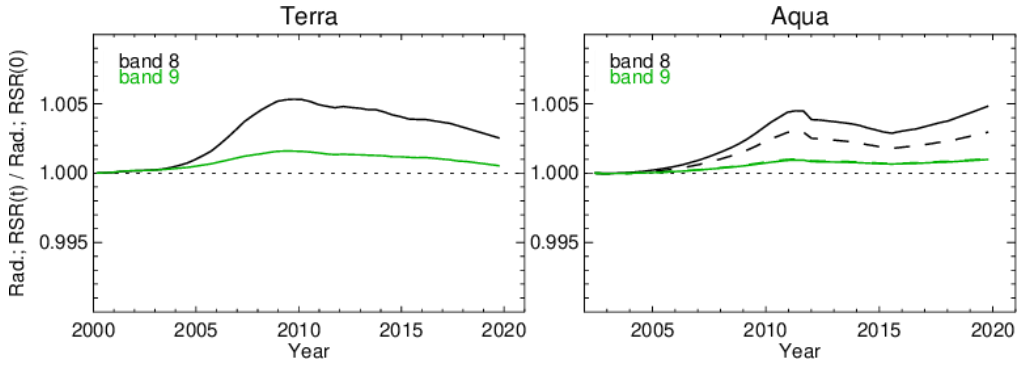

Fig. 7. On-orbit impact of broadband RSR changes on calibrated radiance for Terra (left) and Aqua (right) bands 8 and 9. For Aqua, the solid lines and dashed lines correspond to method 1 and method 2, respectively. Only results for mirror side 1 are shown, but the results for mirror side 2 are similar. The maximum impact for all other VIS/NIR bands is less than 0.1%.

5 Impact of on-orbit RSR changes on RVS characterization

The analysis in Section 4 only considers the on-orbit RSR changes as seen by the SD calibration. However, the on-orbit response changes of both MODIS instruments have significant variation as a function of the AOI of the incoming light off the primary scan mirror. The response variation as a function of AOI is included as the RVS term in Eq. 2. Changes to the RVS are determined on-orbit using a combination of SD data (AOI = 50.2°) and regular lunar observations (AOI = 11.2°). For some bands (Terra bands 1-4, 8-10 and Aqua bands 1-4, 8-9), EV data from pseudo-invariant desert sites are also used to track and calibrate the on-orbit RVS.[3,4] The changing RVS adds two complications to the analysis of the impact of changing RSR on the calibration: the effect of different spectral scenes (lunar, SD, and desert) and the effect that the optical gain, and thus the broadband RSR, has a dependence on AOI. We separately consider the impact of the on-orbit RSR changes on the RVS algorithm that uses the OBC-based approach (lunar and SD only) and the EV-based approach (lunar and desert data).

In the OBC-based RVS algorithm, near-monthly lunar observations made through the SV port are used to derive a long-term trend of the on-orbit gain change at the AOI of the SV. This is compared to the long-term trend of the on-orbit gain change from the SD observations at the SD AOI and a simple linear interpolation is used to derive the relative gain trends (the RVS) at all other AOI. Section 4 showed the results for how the long-term on-orbit gain change from the SD observations would be impacted by the changing broadband RSR. To determine the impact on the OBC-based RVS, we need to also consider the impact on the long-term lunar radiance trend. The lunar radiance trends for each band used in our routine calibration are derived based on a detailed lunar radiance model that takes into account the lunar phase and other considerations using the USGS Robotic Lunar Observatory (ROLO) radiance model.[20,21] In this detailed model, the impact

of the instrument RSR can vary slightly from one lunar observation to the next due to the slight differences in viewing geometry. For simplicity, in this analysis we instead use a single average lunar radiance spectrum to calculate the effect of the time-dependent RSR on the lunar radiance over the missions. The lunar radiance is calculated by multiplying the solar spectrum by a lunar reflectance spectrum calculated by averaging the several years of ROLO model results for Terra lunar observations. We expect this to give a reasonable approximation of the long-term impact of the RSR on the lunar calibration. Similar to our analyses for the SD radiance, we can calculate the impact of the time-dependent RSR on the lunar radiance trend using Eq. 8:

$$R_{rad,moon}(B,t,\theta_{SV}) = \frac{\int RSR(\lambda,B,t,\theta_{SV})L_{moon}(\lambda)d\lambda \,/\, \int RSR(\lambda,B,t,\theta_{SV})d\lambda}{\int RSR_{pl}(\lambda,B)L_{moon}(\lambda)d\lambda \,/\, \int RSR_{pl}(\lambda,B)d\lambda}, \quad (14)$$

where L_{moon} is the lunar radiance spectrum and the viewing angle is the angle of the lunar observations made through the SV port, $\theta_{scan} = \theta_{SV}$.

The OBC-based RVS algorithm is currently used for Terra bands 5-7, 11-19, and 26 and Aqua bands 5-7, 10-19, and 26. For these bands, we evaluate the RSR impact, $R_{rad,moon}$ from Eq. 14, using the time-dependent broadband RSR derived from the scan mirror degradation analysis, Eq. 13. For both instruments, the impact is negligibly small. To get the broadband RSR, we use the optical gain at the AOI of the lunar observations that happen through the SV port. Compared to the previous Section, the only difference is that the total gain term (Fig. 5a and 5b) is taken to be the on-orbit change in $RVS(\theta = \theta_{SV})/m_1$ instead of $1/m_1$, which was valid for the SD AOI. The on-orbit total gain change at the SV AOI can be up to 30% different than at the SD AOI, but the shape of the gain vs. wavelength curve is very similar. However, even with somewhat different values of $RSR_{broadband}$, it remains true that only bands 8 and 9 see any significant impact (>0.1%) due to the changing broadband RSR, and none of the bands using the OBC-based RVS algorithm are impacted.

In the EV-based calibration algorithm, signal trends from various viewing angles of pseudo-invariant calibration sites in the Libya desert are used in combination with the lunar observations to derive trends of on-orbit gain change across all AOI. This algorithm is applied in C6.1 L1B to Aqua and Terra bands 1-4, 8-9, and Terra band 10. For the EV-based bands, the desert data are used instead of the SD data to track the on-orbit gain change at the SD AOI, due to concerns about the accuracy of the SD calibration especially for the short-wavelength VIS bands. The initial on-orbit SD calibrations are still used for the absolute reflectance and radiance calibration. In practice, trends of the signals from the desert sites at several different AOI are corrected for site BRDF and instrument temperature and fit over time and AOI to derive a smooth function of the on-orbit gain change. For the fitting over AOI, the fit is constrained to the lunar data trend at the SV AOI since the lunar data are expected to be accurate and have lower uncertainty than the desert data.

For the desert scene, we can calculate the impact of the time-dependent RSR on the radiance trend using Eq. 8 where $L_{scene} = L_{desert}$ is a typical TOA desert radiance spectrum taken from MODTRA simulations.[22] The broadband RSR impact depends on the viewing angle of the desert site, or equivalently the AOI of the Earth-reflected light off the scan mirror. For a single MODIS scan, the AOI varies from 10.5° to 65.5° from the beginning to the end of scan and the on-orbit change in the optical gain can vary significantly over this range, especially for the short wavelength bands. We calculate the optical gain and the broadband RSR as a function of time at a series of different values of AOI covering this full range, and then use these $RSR_{broadband}$ functions to calculate the RSR impact, $R_{rad,desert}$, when viewing the desert scene. The results for Terra and Aqua bands 8 and 9 are shown in Fig. 11 along with the broadband RSR impact on the lunar scene calculated using the $RSR_{broadband}$ at the SV AOI of 11.2°. As was the case in Section 4 for the SD calibration, the impact is largest for band 8 of both instruments, somewhat smaller for band 9,

and negligible for all other bands, and the impact is smaller for Aqua method 2 compared to method 1.

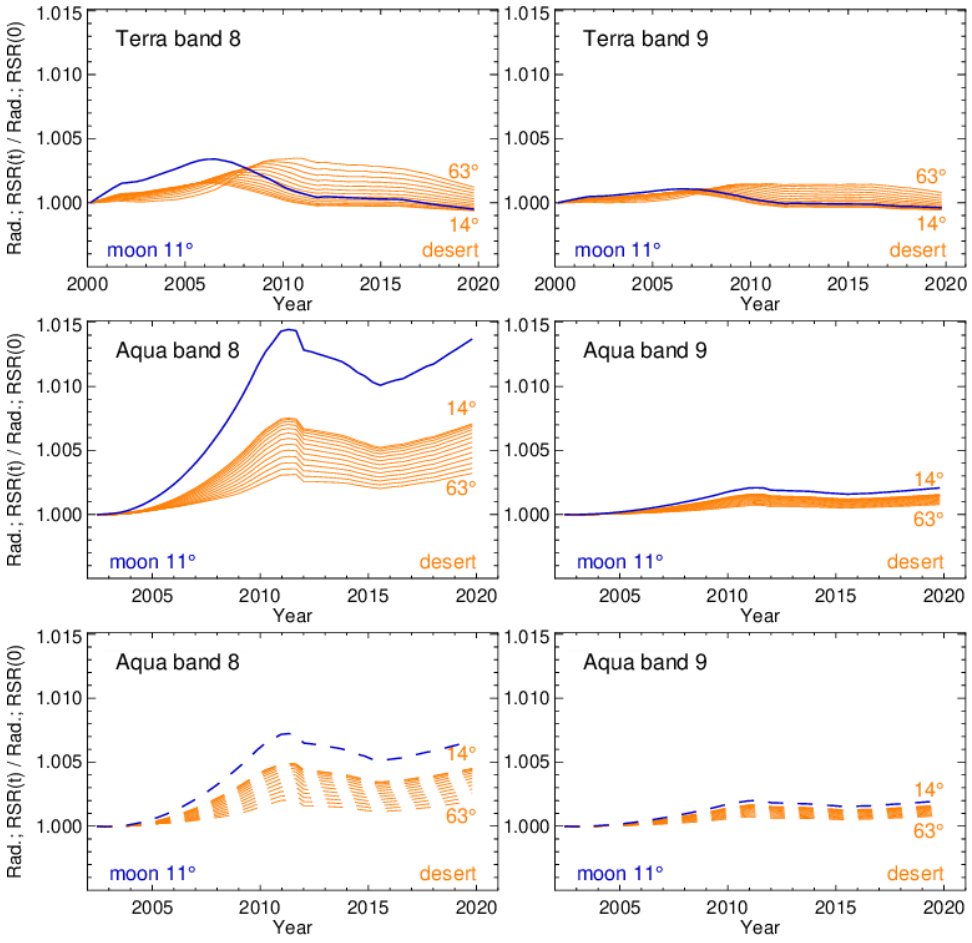

Fig. 8. On-orbit impact of broadband RSR changes on calibrated radiance for bands 8 and 9 for Terra (top row), Aqua method 1 (middle row), and Aqua method 2 (bottom row). The impact for the lunar scene at the SV AOI is shown in blue. The impacts for the desert scene at different AOI are shown as a series of orange lines which correspond to 13 evenly spaced AOI from 14° to 63° as indicated in the plots. Only results for mirror side 1 are shown. The maximum impact for all other VIS/NIR bands is less than 0.1%.

Clearly, Aqua band 8 method 1 sees the largest impact of the changing RSR of any of the bands that use the EV-based calibration algorithm. The maximum impact varies from 0.3% to 0.8% over the range of AOI for the desert scene and is up to 1.4% for the lunar scene. The differences seen with AOI for the desert curves are simply a result of the RSR dependence on AOI, but the

discrepancies between the desert and lunar data at the same AOI are due to the differences in the spectral properties of the two scenes. We routinely monitor the long-term lunar radiance and desert radiance trends at the same AOI, calculated with the current C6.1 algorithm that does not include RSR, and find them to be in good agreement. If the method 1 RSR is accurate, there should be a 0.6% divergence between these lunar and desert trends for Aqua MODIS band 8, whereas the divergence would only be 0.2% if the method 2 RSR is accurate. This may indicate that the method 2 RSR is closer to the truth, but the one standard deviation statistical uncertainty of the desert observations is typically around 1% even after BRDF correction, so even a 0.6% divergence may still be too small to observe conclusively. In the C6/6.1 calibration algorithm, we fix the calibration to the lunar trend at the SV AOI, so in the worst case the error in the current m_1/RVS calibration for Aqua band 8 due to ignoring the time-dependent RSR effects could be up to 1.4% at the beginning of scan, dropping to only about 0.3% at the end of scan.

6 Impact of on-orbit RSR changes on Earth scene products

6.1 Earth scene radiance dependence

The impact of on-orbit RSR changes on the retrieved EV scene radiance is of significant interest as this is the primary goal of the calibration and it has the potential to impact the downstream products derived from the NASA L1B. In addition, for narrow-band multi-spectral instruments like MODIS, there is considerable interest in understanding the role of the RSR when making comparisons to other multi-spectral or hyper-spectral instruments, both satellite-based and ground-based, for the purpose of intercomparison and cross-calibration.[23,24] Changes in the on-orbit RSR can make these comparisons more challenging.

The focus in this paper so far has been to provide a quantitative measure of the calibration biases that exist in the current C6/6.1 L1B radiances due to the effects of the time-dependent RSR. If an improved L1B calibration were to be implemented, including the adjustments for the time-dependent RSR, these calibration biases would be removed. It should be stressed though, that the bias of the time-dependent RSR on the Earth scene retrieval would still be present in the improved L1B products. For example, if MODIS band 1 is used to observe a desert scene with a pseudo-invariant radiance spectrum $L_{desert}(\lambda)$, the MODIS-measured radiance $\overline{L_{desert}(B)}$ would be expected to have a slight drift in time due to the time-dependence of the RSR (see Eq. 7). In the current C6.1 L1B, desert scenes are primarily used to derive the calibration parameters for band 1, so the retrieved C6.1 L1B radiance over a similar desert scene should not have any drift, since the calibration bias and the Earth retrieval bias cancel each other out. But if band 1 is viewing a different scene, both the calibration bias and the Earth scene retrieval bias would have to be considered to uncover the true radiance of the scene, $L_{scene}(\lambda)$. In an improved L1B product, the calibration biases can be removed, but the Earth retrieval biases can obviously not be removed in a general way, since they depend on the properties of the scene.

As a further example, we calculate the impact of the time-dependent RSR on the radiance for a few typical Earth scenes (desert, ocean, cloud) for some of the bands that have the most significant time-dependent RSR. Figure 9 shows the results for band 8 of Aqua MODIS for the broadband RSR changes at nadir AOI. The typical Earth scene spectra are TOA spectra from MODTRAN simulations.[22] While these may not be the most quantitatively relevant examples for MODIS higher level data products, they provide a reasonable example of how the impact of the changing RSR can depend significantly on the details of the spectral radiance for different scenes. Once again, the variation in the impact between different scenes is smaller for method 2 compared

to method 1. For Aqua band 8 only, the most recent version of the NASA ocean color products includes corrections for the time-dependent RSR using the method 1 RSR and assuming a typical ocean scene spectra,[8] but note that these corrections are applied directly to the ocean color products and are not included in the NASA Level 1 products.

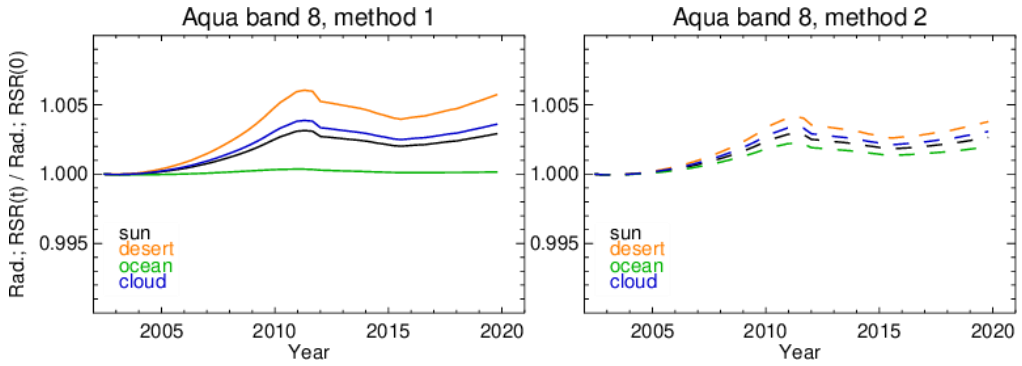

Fig. 9. On-orbit impact of broadband RSR changes on calibrated Earth scene radiance for different scenes for Aqua MODIS band 8 at nadir AOI for method 1 (solid lines) and method 2 (dashed lines). For comparison, the solar spectral scene is also included.

6.2 Potential implementation in L1B

As stated in the Introduction, the out-of-band RSR and on-orbit changes to the RSR are not currently considered in NASA's L1B products for MODIS. Here we provide a description of how the L1B products would have to be defined and updated if the RSR effects were to be included in future MODIS L1B Collections. The reflectance factor and radiance products would be defined in the same way as in Eqs. 1 and 2, with the exception that the $\overline{E_{sun}}$ term defined in Eq. 4 would have a time and scan angle dependence due to the time and scan angle dependence of the RSR.

For practical convenience, the calibration could be derived first using the static pre-launch RSR, with the corrections for the time-dependent RSR added as a final step. The SD calibration would first be calculated using the pre-launch merged IB/OOB RSR as in Section 2. Then the rest of the calibration algorithm would be executed using the current calibration method. The time-

dependent optical gain and broadband RSR (Eq. 13) would be calculated as a function of scan angle. The final time-dependent and angle-dependent RSR would then be used to calculate the calibration bias in the m_1 and RVS values, and this bias would be removed from the initial calibration to provide a final set of m_1 and RVS look-up-tables (LUTs). The $\overline{E_{sun}}$ values, which are currently a fixed LUT in the L1B, would need to be provided for each band as a two-dimensional LUT covering a series of AOI and time stamps throughout the mission. This methodology can be considered for implementation in future versions of NASA MODIS L1B products. The methodology is similar to that currently used for the NASA L1B products for SNPP VIIRS, which has a time-dependent RSR,[6] but MODIS would have the additional complication of a scan angle dependent RSR.

7 On-orbit changes to in-band RSR

Finally, we review the changes to the in-band RSR that are directly measured on-orbit by the SRCA and investigate the impact to the RSB calibration and Earth scene products. Operated in spectral mode, the SRCA is designed to scan over most of the IB wavelength range of each of the MODIS bands and measure the RSR of each detector. Detailed descriptions of the SRCA's spectral operation and algorithm have been presented before,[10] as well as results from on-orbit calibrations.[11,12] The SRCA spectral mode has been operated multiple times per year over the course of both Terra and Aqua MODIS missions, providing a significant amount of data to track the RSR changes.

Figure 10 shows examples of the IB RSR changes as measured by the SRCA at select times in the mission for select bands of Terra and Aqua MODIS. For Aqua MODIS, all of the bands with acceptable data quality show no significant change in the shape of the in-band RSR with time. For Terra MODIS, several of the bands show significant on-orbit changes in the shape of the in-band

RSR, including bands 1 and 19 shown in Fig. 10. We do not know the root cause for the observed Terra MODIS in-band RSR changes, but one possibility is degradation of the bandpass filters located in front of the MODIS detector arrays. Note that for both instruments we do not consider the SRCA spectral results of bands 2, 3, 8, or 9 in any of this analysis. The results for band 2 may be accurate but are typically not reported due to a difference in the SRCA configuration used for the pre-launch vs on-orbit measurements.[9] The results for bands 3, 8, and 9 are reliable for early mission calibrations, but due to SRCA lamp failures and scan mirror degradation, the signal-to-noise ratio of the SRCA spectral results is too low to provide reliable results throughout the missions. The measurements in Fig. 10 are the average over all detectors within a band; the results are generally consistent for all detectors within a band, including in the cases where on-orbit changes are observed. The on-orbit changes are also observed to be equal for both mirror sides of the MODIS scan mirror.

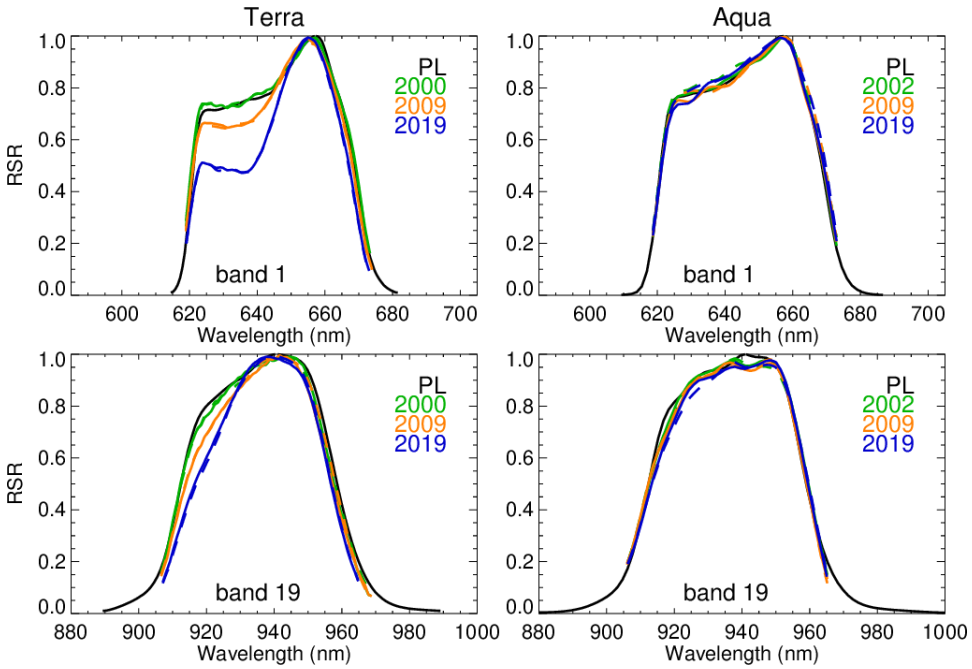

Fig. 10. Examples of in-band RSR for select bands of Terra (left column) and Aqua (right column) MODIS at select times (years) in the mission. The solid lines represent mirror side 1 results and the dashed lines represent mirror side 2 results. The pre-launch data are from measurements made with the SpMA.

Note that if the broadband RSRs calculated in the previous Sections are an accurate representation of the on-orbit RSR changes, the in-band portion of the broadband RSR change should in principle be measured by the SRCA, so it is reasonable to ask whether the SRCA measurements agree with the broadband RSR calculation. Unfortunately, the variation of the SRCA measurements from one spectral calibration to the next is generally larger than the in-band RSR changes that would be expected from the broadband RSR calculation. The short-wavelength blue bands are the bands that see the largest broadband RSR change, but these are also the bands that have the lowest signal-to-noise ratio in the SRCA measurements.

To quantify the in-band RSR changes like those shown in Fig. 10, we consider the effect of these RSR changes on the on-orbit trends of the calibrated reflectance and radiance. This calculation is more challenging with the SRCA results than it was with the broadband RSR analysis since the SRCA only tracks the on-orbit changes in RSR over the in-band part of the spectra, and we don't have any accurate way to merge this changing in-band RSR with the OOB RSR. As a very rough approximation, we perform this merging by simply replacing the pre-launch RSR measurement with the SRCA measurement over the valid SRCA measurement range for each SRCA spectral mode calibration, i.e.

$$RSR(\lambda, B, t) = \begin{cases} RSR_{pl}(\lambda, B) & \lambda \; outside \; SRCA \; measurement \; range \\ RSR_{SRCA}(\lambda, B, t) & \lambda \; inside \; SRCA \; measurement \; range \end{cases}. \quad (15)$$

By merging the in-band SRCA spectral results with the pre-launch OOB spectral results, we are making the implicit assumption that the maximum optical transmittance is unchanged relative to the magnitude of the OOB spectrum, which is not necessarily true. The changes observed by the SRCA for Terra MODIS are possibly due to changes to the narrow band filters located in front of

the MODIS detectors. Degradation of the scan mirror and other optics is less likely to induce sharp features, such as those shown in Fig. 10 for Terra band 1. Large changes to the in-band transmission of these filters may very likely be correlated with large changes in the OOB transmission of these filters, which we have no way of tracking on orbit, adding significant uncertainty in the attempts to characterize the on-orbit effects of the OOB RSR. However, by assuming a fixed OOB RSR as in Eq. 15, we can get an approximate assessment of the relative impact of the measured IB RSR changes.

Using this time-dependent RSR from Eq. 15 for each SRCA spectral calibration, we calculate the ratio $R_{rad,SD}(B,t)$ from Eq. 10. Since both the SD degradation $\Delta_{SD}(\lambda)$ and the solar spectrum $E_{sun}(\lambda)$ change slowly over the wavelength ranges of the narrow MODIS bands, the changing in-band RSR has a minimal effect on either the reflectance or radiance. The results for the effect of in-band RSR changes on the calibrated radiance are shown for Terra MODIS in Fig. 11. Band 1 sees the largest effect, up to 0.4%, due to its relatively large bandwidth and relatively large on-orbit RSR change. For Aqua MODIS, the on-orbit trends are less than for Terra and are less than 0.1% over the mission for all bands.

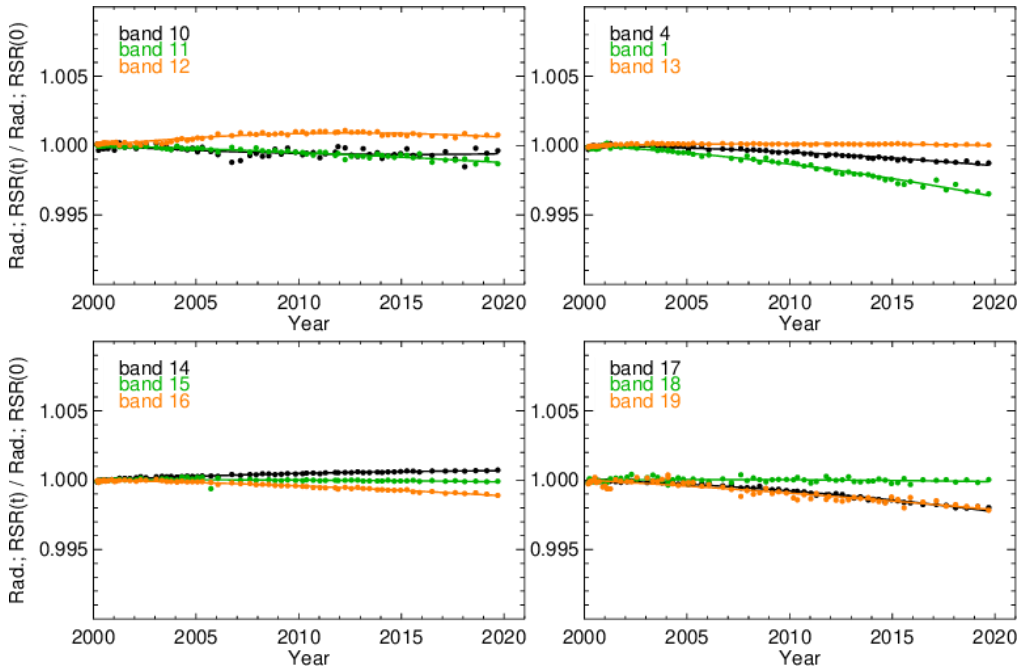

Fig. 11. On-orbit impact of IB RSR changes on calibrated radiance, normalized to the mission start, $R_{rad,SD}(B,t)/R_{rad,SD}(B,t_0)$, for Terra VIS/NIR bands. Each point represents an SRCA spectral calibration and the lines are quadratic fits to the data.

While the effects of the in-band RSR changes are found to be small for the reflectance and radiance in the SD-based calibration, the effect on the EV products depends greatly on the spectral properties of the EV scene radiance. Similar to Section 6.1, we calculate the impact of the changing in-band RSR on the radiance for different scenes using Eq. 8. The results are shown in Fig. 12 for Terra bands 1, 4, 17, and 19, which have the largest impact. For bands 1, 4, and 17, the spread between the results from different scenes is within a few tenths of a percent. For the water absorption band 19, there are sharp changes in the MODTRAN spectral profile within the bandwidth, so the gradual narrowing of the bandwidth on-orbit results in a several percent change in the retrieved radiance. This demonstrates how a changing in-band RSR could result in significant scene-dependent impacts even though the MODIS RSB bandwidths are relatively narrow.

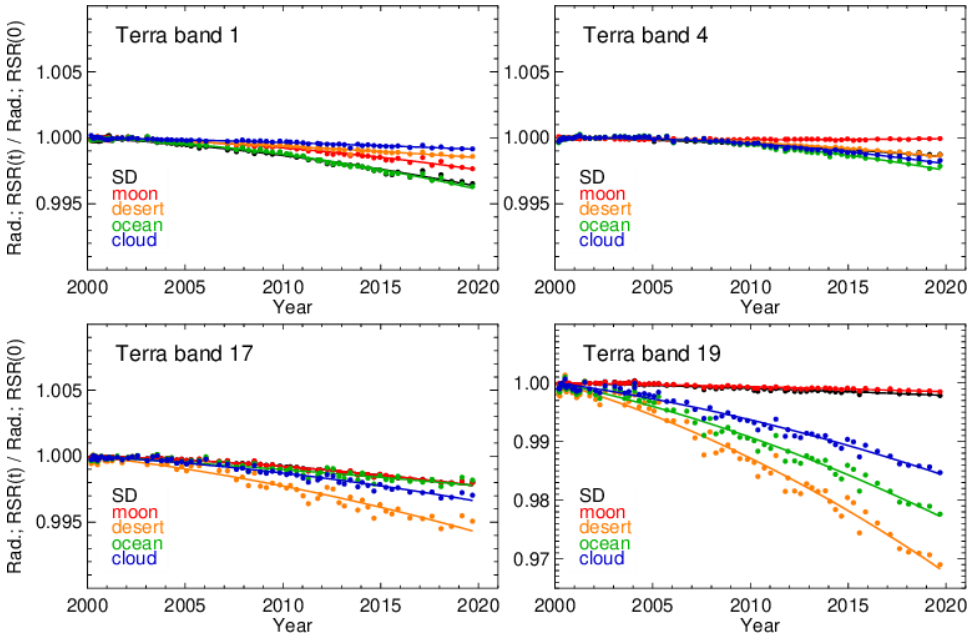

Fig. 12. On-orbit impact of in-band RSR changes on calibrated radiance, normalized to mission start, for different scenes for Terra MODIS bands 1, 4, 17, and 19. Each point represents an SRCA spectral calibration and the lines are quadratic fits to the data. Note the different vertical scale for band 19.

Due to the lack of a reliable method for combining the IB RSR changes from the SRCA measurements with the pre-launch or on-orbit broadband RSR, we would not recommend using the SRCA results in the L1B calibration. The results presented here show that the IB RSR is very stable on-orbit, though there may be some exceptions for specific Terra MODIS bands when viewing specific scenes. Clearly, any products that rely on long-term trends of the Terra MODIS water absorption bands may need to consider the effects of the changing in-band RSR to produce accurate results.

8 Summary

In summary, this paper considers the impacts to both the Terra and Aqua MODIS reflective solar band calibrations due to the out-of-band and the time-dependent relative spectral responses for each band. Since the current and all previous MODIS L1B Collections use only the pre-launch IB

RSR when calibrating the RSB, there would be a modest impact on the calibrated radiance if the calibration were changed to use both the pre-launch IB and OOB RSR measurements: up to 0.7% for Terra MODIS and up to 0.7% or 1.5% for Aqua MODIS depending on the version of pre-launch RSR. Two methods are presented to track on-orbit RSR changes: estimating the modulated OOB RSR due to broadband instrument degradation, and using the on-board SRCA to directly measure the in-band RSR changes. The impacts of time-dependent RSR changes on the long-term trends of the calibrated radiance are generally small in most cases. The impact on the SD-based calibration is in the 0.1% to 0.5% range for Terra bands 1, 4, 8, 9, 17, and 19, and Aqua bands 8 and 9, and is negligible for all other bands. After considering the use of the lunar and desert scene data in the calibration of the on-orbit RVS, the calibration error for Aqua band 8 may be larger, up to 1.4% for viewing angles near the beginning of scan, depending on the version of pre-launch RSR that is used. The impact on the reflectances is generally less than the impact on the radiances.

While the SRCA measurements are expected to be fairly accurate,[13] the broadband RSR results carry a great deal of uncertainty since they are based on the assumption that the broadband degradation of the primary scan mirror is the only factor driving the on-orbit RSR changes. This assumption is particularly suspect for Terra MODIS, where the mechanisms of on-orbit degradation are less well understood. The accuracy of the results is of course also highly dependent on the accuracy of the pre-launch OOB RSR measurements. Two different versions of pre-launch OOB RSR were provided by the instrument vendor for Aqua MODIS, and the calculated on-orbit impacts of the OOB RSR vary greatly between the two versions.

We present a methodology for including the corrections for time-dependent braodband RSR in the L1B calibration for both MODIS instruments and this could potentially be considered for inclusion in future MODIS Collections. Importantly, a changing RSR can have a significant effect

on Earth scene radiance retrieval even if the effect on the calibration is removed. Observations of Earth scenes that have significant spectral features within the bandwidth of one of the MODIS bands could be significantly impacted by modest changes of the in-band RSR of these bands. The large in-band changes seen for the Terra water absorption band 19 may be of particular concern.

Acknowledgments

We thank Daniel Link and Emily Aldoretta for their work on SRCA calibration analysis, Na Chen for her work on electronic calibration analysis, and Aisheng Wu for providing MODTRAN spectral profiles. We also thank Truman Wilson for his review of this paper. This manuscript is an extension of an SPIE conference proceedings paper: Kevin A. Twedt, Amit Angal, Xiaoxiong Xiong, "Effects of time-varying relative spectral response on the calibration of MODIS reflective solar bands", Proc. SPIE 10764, Earth Observing Systems XXIII, 1076413 (7 September 2018); doi: 10.1117/12.2321255

References

[1] Barnes, W. L. and Salomonson, V. V., "MODIS: a global imaging spectroradiometer for the Earth Observing System," Proc. SPIE **10269**, 102690G (1992).
[2] Xiong, X., Barnes, W. L., Guenther, B. and Murphy, R. E., "Lessons learned from MODIS," Adv. Space Res. **32**(11), 2107–2112 (2003).
[3] Sun, J., Xiong, X., Angal, A., Chen, H., Wu, A. and Geng, X., "Time-Dependent Response Versus Scan Angle for MODIS Reflective Solar Bands," IEEE Trans. Geosci. Remote Sens. **52**(6), 3159–3174 (2014).
[4] Xiong, X., Angal, A., Twedt, K. A., Chen, H., Link, D., Geng, X., Aldoretta, E. and Mu, Q., "MODIS Reflective Solar Bands On-Orbit Calibration and Performance," IEEE Trans. Geosci. Remote Sens. **57**(9), 6355–6371 (2019).
[5] Barnes, W. L., Pagano, T. S. and Salomonson, V. V., "Prelaunch characteristics of the Moderate Resolution Imaging Spectroradiometer (MODIS) on EOS-AM1," IEEE Trans. Geosci. Remote Sens. **36**(4), 1088–1100 (1998).
[6] Lei, N., Xiong, X. and Guenther, B., "Modeling the Detector Radiometric Gains of the Suomi NPP VIIRS Reflective Solar Bands," IEEE Trans. Geosci. Remote Sens. **53**(3), 1565–1573 (2015).
[7] Lee, S. and Meister, G., "MODIS Aqua Optical Throughput Degradation Impact on Relative Spectral Response and Calibration of Ocean Color Products," IEEE Trans. Geosci. Remote Sens. **55**(9), 5214–5219 (2017).
[8] Lee, S., Meister, G. and Franz, B., "MODIS Aqua Reflective Solar Band Calibration for NASA's R2018 Ocean Color Products," Remote Sens. **11**(19), 2187 (2019).

[9] Choi, T., Xiong, X., Wang, Z. and Link, D., "Terra and Aqua MODIS on-orbit spectral characterization for reflective solar bands," Proc. SPIE **8724**, 87240Y (2013).
[10] Montgomery, H., Che, N., Parker, K. and Bowser, J., "The algorithm for MODIS wavelength on-orbit calibration using the SRCA," IEEE Trans. Geosci. Remote Sens. **38**(2), 877–884 (2000).
[11] Xiong, X., Che, N. and Barnes, W. L., "Terra MODIS on-orbit spectral characterization and performance," IEEE Trans. Geosci. Remote Sens. **44**(8), 2198–2206 (2006).
[12] Link, D., Wang, Z., Twedt, K. A. and Xiong, X. J., "Status of the MODIS spatial and spectral characterization and performance after recent SRCA operational changes," Proc. SPIE **10402**, 104022G, SPIE (2017).
[13] Aldoretta, E. J., Link, D., Twedt, K. A. and Xiong, X., "Assessment of the on-orbit MODIS SRCA spectral uncertainty," Proc. SPIE **10764**, 1076412 (2018).
[14] Xiong, X., Chiang, K.-F., Adimi, F., Li, W., Yatagai, H. and Barnes, W. L., "MODIS correction algorithm for out-of-band response in the short-wave IR bands," Proc. SPIE **5234**, 605 (2004).
[15] Wilson, T. M. and Xiong, X., "Subsample difference correction for Terra MODIS SWIR bands 5-7 using lunar observations," Proc. SPIE **10785**, 107851B (2018).
[16] Chen, H., Xiong, X., Angal, A. and Twedt, K. A., "On-Orbit Characterization of the MODIS SDSM Screen for Solar Diffuser Degradation Estimation," IEEE Trans. Geosci. Remote Sens. **55**(11), 6456–6467 (2017).
[17] Geng, X., Angal, A., Li, Y., Twedt, K. A. and Xiong, X., "Improvements in the on-orbit response versus scan-angle characterization for the MODIS ocean color bands," Proc. SPIE **11151**, 1115124 (2019).
[18] Angal, A., Geng, X., Xiong, X., Twedt, K. A., Wu, A., Link, D. O. and Aldoretta, E., "On-Orbit Calibration of Terra MODIS VIS Bands Using Polarization-Corrected Desert Observations," IEEE Trans. Geosci. Remote Sens. (2020).
[19] Xiong, X., Chen, N., Li, Y. and Wilson, T., "Assessments and applications of Terra and Aqua MODIS on-orbit electronic calibration," Proc. SPIE **9972**, 99720X (2016).
[20] Sun, J.-Q., Xiong, X., Barnes, W. L. and Guenther, B., "MODIS Reflective Solar Bands On-Orbit Lunar Calibration," IEEE Trans. Geosci. Remote Sens. **45**(7), 2383–2393 (2007).
[21] Kieffer, H. H. and Stone, T. C., "The Spectral Irradiance of the Moon," Astron. J. **129**(6), 2887–2901 (2005).
[22] Berk, A., Bernstein, L. S., Anderson, G. P., Acharya, P. K., Robertson, D. C., Chetwynd, J. H. and Adler-Golden, S. M., "MODTRAN Cloud and Multiple Scattering Upgrades with Application to AVIRIS," Remote Sens. Environ. **65**(3), 367–375 (1998).
[23] Thome, K. J., Czapla-Myers, J. S. and Biggar, S. F., "Vicarious calibration of Aqua and Terra MODIS," Proc. SPIE **5151**, 395 (2003).
[24] Chander, G., Mishra, N., Helder, D. L., Aaron, D. B., Angal, A., Choi, T., Xiong, X. and Doelling, D. R., "Applications of Spectral Band Adjustment Factors (SBAF) for Cross-Calibration," IEEE Trans. Geosci. Remote Sens. **51**(3), 1267–1281 (2013).